Journal of Macromolecular Science, Part A
Publication details, including instructions for authors and subscription information:
http://www.informaworld.com/smpp/title~content=t713597274

Effect of $CaCO_3$ Filler Component on Solid State Decomposition Kinetic of PP/LDPE/$CaCO_3$ Composites

Kamil Şrn[a]; Fatih Doğan[b]; Mehmet Balcan[c]; İsmet Kaya[d]
[a] Faculty of Science and Arts, Department of Chemistry, Celal Bayar University, Manisa, Turkey [b] Faculty of Education, Secondary Science and Mathematics Education, Çanakkale Onsekiz Mart University, Çanakkale, Turkey [c] Faculty of Science, Department of Chemistry, Ege University, Bornova, Turkey [d] Faculty of Science and Arts, Department of Chemistry, Çanakkale Onsekiz Mart University, Çanakkale, Turkey

To cite this Article Şrn, Kamil , Doğan, Fatih , Balcan, Mehmet and Kaya, İsmet(2009) 'Effect of $CaCO_3$ Filler Component on Solid State Decomposition Kinetic of PP/LDPE/$CaCO_3$ Composites', Journal of Macromolecular Science, Part A, 46: 10, 949 — 958
To link to this Article: DOI: 10.1080/10601320903158297
URL: http://dx.doi.org/10.1080/10601320903158297

Journal of Macromolecular Science®, Part A: Pure and Applied Chemistry (2009) **46**, 949–958

ISSN: 1060-1325 print / 1520-5738 online
DOI: 10.1080/10601320903158297

Taylor & Francis
Taylor & Francis Group

Effect of $CaCO_3$ Filler Component on Solid State Decomposition Kinetic of PP/LDPE/$CaCO_3$ Composites

KAMIL ŞİRİN[1,*], FATIH DOĞAN[2], MEHMET BALCAN[3] and İSMET KAYA[4]

[1]*Celal Bayar University, Faculty of Science and Arts, Department of Chemistry, 45100, Manisa, Turkey*
[2]*Çanakkale Onsekiz Mart University, Faculty of Education, Secondary Science and Mathematics Education 17100, Çanakkale, Turkey*
[3]*Ege University, Faculty of Science, Department of Chemistry, 35100, Bornova, Turkey*
[4]*Çanakkale Onsekiz Mart University, Faculty of Science and Arts, Department of Chemistry, 17100, Çanakkale, Turkey*

Received March 2009, Accepted April 2009

In this study, the effect of addition Calcium carbonate ($CaCO_3$) filler component on solid state thermal decomposition procedures of Polypropylene-Low Density Polyethylene (PP-LDPE; 90/10 wt%) blends involving different amounts (5, 10, 20 wt%) Calcium carbonate ($CaCO_3$) was investigated using thermogravimetry in dynamic nitrogen atmosphere at different heating rates. An integral composite procedure involving the integral iso-conversional methods such as the Tang (TM), the Kissinger-Akahira-Sunose method (KAS), the Flynn-Wall-Ozawa (FWO), an integral method such as Coats-Redfern (CR) and master plots method were employed to determine the kinetic model and kinetic parameters of the decomposition processes under non-isothermal conditions. The Iso-conversional methods indicated that the thermal decomposition reaction should conform to single reaction model. The results of the integral composite procedures of TG data at various heating rates suggested that thermal processes of PP-LDPE-$CaCO_3$ composites involving different amounts of $CaCO_3$ filler component (5, 10, 20 wt%) followed a single step with approximate activation energies of 226.7, 248.9, and 252.0 kJ.mol^{-1} according to the FWO method, respectively and those of 231.3, 240.1 and 243.0 kJ mol^{-1} at 5°C min^{-1} according to the Coats-Redfern method, the reaction mechanisms of all the composites was described from the master plots methods and are P_n model for composite C-1, R_n model for composites C-2 and C-3, respectively. It was found that the thermal stability, activation energy and thermal decomposition process changed by the increasing $CaCO_3$ filler weight in composite structure.

Keywords: $CaCO_3$, polypropylene, low density polyethylene, kinetic method, mechanism function

1 Introduction

Polypropylene (PP) and polyethylene (PE) blends have been attracting a lot of attention because of various reasons. One of the reasons is the cost-effectiveness of these blends in industrial and commercial usage. Polymer blending can be done at a relatively low cost using an extruder. Production of new polymers, on the other hand, requires capital intensive plants and reactors that must operate on a reasonably large scale for reasons of economics (1).

Polypropylene has excellent electrical and insulating properties, chemical inertness, and moisture resistance when it is used in room-temperature applications. It is relatively stiff and has a high melting point, low density, and relatively good resistance to impact (2–4). PP has found a wide range of applications in the household goods, packaging, and automobiles. Polypropylene is used in applications ranging from injection-molded and blow-molded products and fibers and filaments to films and extrusion coatings (4–6).

Low density polyethylene (LDPE) has a wide application field in industry. Because of the suitable properties, it can be processed easily and used different materials. Polyethylene has an excellent chemical resistance and is not attacked by acids, bases, or salts (5–9). Low-density polyethylene is a partially crystalline solid with a degree of crystallinity in the 50 to 70% range, melting temperature of 100–120°C, and specific gravity of about 0.91 to 0.94 g cm^{-1} (5–8).

Composite material is a material system consisting of a mixture or combination of two or more micro-constituents mutually insoluble and differing in form and/or material composition. Particulate-filled thermoplastic composites have proved to be of significant commercial importance in recent years, as industrialists and technologists have sought to find new and cost-effective materials for specific applications (10–12). Calcium carbonate ($CaCO_3$) is one of the

* Address corresponence to: Kamil Şirin, Celal Bayar University, Faculty of Science and Arts, Department of Chemistry, 45100, Manisa, Turkey. Tel.: +90 2862180018; Fax: +90 2862180018; E-mail: sirin.kamil@gmail.com

most commonly used inorganic fillers in thermoplastics. Importantly, the use of calcium carbonate allows the association of a rigid and resistant material, which does not cost too much, with many polymers including polyolefines (10–14).

The focus of this study is to understand the changes on thermal decomposition mechanism and kinetic parameters of PP-LDPE (90/10 wt%) blend when different ratios of 5, 10, 20 wt% $CaCO_3$ are added. The kinetics of the thermal degradation of these composites is carried out by using thermogravimetry. The activation energy of thermal degradation of $CaCO_3$ composite with N_2 was obtained by Tang, KAS, FWO, and CR methods. Thermal degradation mechanism for $CaCO_3$ composite was investigated by CR method, master plots method.

2 Experimental

2.1 Materials

Isotactic polypropylene (PP-MH418) and Low-density polyethylene (LDPE-I 22-19 T) were supplied as pellets by Petkim Petrochemical Company (Aliaga, Izmir, Turkey). The number-average molecular weight (*M*n), weight-average molecular weight (*M*w) and polydispersity index (PDI) values of PP and LDPE homopolymer were 20300, 213600 g.mol^{-1} and 10.5, and 29600, 157000 g.mol^{-1} and 5.3, respectively. The specific gravity of the PP-MH418 is 0.905 g cm^{-3} and that of the LDPE-I 22-19 T is 0.919-0.923 g cm^{-3}, with melt flow index of 4–6 g 10 min^{-1} (2.16 kg, 230 ± 0.5 °C) and 21–25 g.10 min^{-1} (2.16 kg, 190 ± 0.5°C), respectively. Calcium carbonate filler (AS 0884 PEW) with particle size 20 μ m was provided by Tosaf Company (Israel).

2.2 Preparation of Blends

Polypropylene-Low Density Polyethylene (PP-LDPE) blends involving (PP/LDPE; 90/10 wt%.) with different amounts (5, 10, 20 wt%.) Calcium carbonate ($CaCO_3$) was prepared by melting-blend with a single-screw extruder (Collin E 30P). The blends were prepared by melting the mixed components in an extruder which was set at the extruder diameter: 30 mm, length to diameter ratio: 20, pressure: 9–10 bar, temperature scale composites from filing part to head were 190–250°C and screw operation speed: 30 rev.min^{-1}. All compounds were produced as 70 μm thick and 10 cm wide films. Composites ratio were prepared and their codes are given in Table 1. These composites are called as composite-1 (C-1), composite-2 (C-2), and composite-3 (C-3). All of these composites were prepared as samples weighing 1000 grams, while keeping the 90/10 PP-LDPE ratio constant.

Table 1. Nomenclature, components and composition of composites

	Composition, wt%		
Sample Code	*PP*	*LDPE*	*$CaCO_3$*
C-1	90	10	5
C-2	90	10	10
C-3	90	10	20

2.3 Measurements

Thermal data were obtained by using Perkin Elmer Diamond Thermal Analysis. The TG-DTA measurements were made within the 15–1000°C range, operating in dynamic mode, with the following conditions; sample weight ~5 mg, heating rates 5, 10, 15 and 20°C.min^{-1}, atmosphere of nitrogen (10 cm^3.min^{-1}), and sealed platinum pan. The infrared spectra were measured by Perkin7-Elmer Spectrum One FT-IR system. The FT-IR spectra were recorded using a universal ATR sampling accessory within the wavelengths of 4000–550 cm^{-1}.

2.4 Kinetics Methods

The application of dynamic TG methods holds great promise as a tool for unraveling the mechanisms of physical and chemical processes that occur during polymer degradation. In this paper, integral isoconversional methods were used to analyze the non-isothermal kinetics of all the C-1, C-2 and C-3.

The rate of solid-state non-isothermal decomposition reactions is expressed as:

$$\frac{d\alpha}{dT} = \left(\frac{A}{\beta}\right) \exp\left(\frac{-E}{RT}\right) f(\alpha) \qquad (1)$$

Rearranging Equation 1 and integrating both sides of the equation leads to the following expression:

$$g(\alpha) = \left(\frac{A}{\beta}\right) \int_{T_0}^{T} \exp\left(\frac{-E}{RT}\right) dT = \left(\frac{AE}{\beta\, R}\right) p(u) \qquad (2)$$

Where $p(u) = \int_{\infty}^{u} -(\frac{e^{-u}}{u^2})\, du$ and $u = \mathrm{E/RT}$.

2.4.1. *Flynn-Wall-Ozawa method (15–16)*

This method is derived from the integral method. The technique assumes that the $A, f(\alpha)$ and E are independent of T while A and E are independent of α , then Equation 2 may be integrated to give the following in logarithmic form:

$$\log g(a) = \log(AE/R) - \log\beta + \log\ \mathrm{p}(E/RT) \qquad (3)$$

Using Doyle's approximation (17) for the integral which allows for $E/RT > 20$, Equation 3 now can be simplified as:

$$\log\beta = \log(AE/R) - \log g(a) - 2.315 - 0.4567\, E/RT \qquad (4)$$

Table 2. Algebraic expression for the most frequently used mechanisms of solid state process

No	*Mechanisms*	*Symbol*	*Differential form, $f(\alpha)$*	*Integral form, $g(\alpha)$*
		Sigmoidal curves		
1	N and G (n = 1)	A_1	$(1-\alpha)$	$[-\ln(1-\alpha)]$
2	N and G (n = 1.5)	$A_{1.5}$	$(3/2)(1-\alpha)[-\ln(1-\alpha)]^{1/3}$	$[-\ln(1-\alpha)]^{2/3}$
3	N and G (n = 2)	A_2	$2(1-\alpha)[-\ln(1-\alpha)]^{1/2}$	$[-\ln(1-\alpha)]^{1/2}$
4	N and G (n = 3)	A_3	$3(1-\alpha)[-\ln(1-\alpha)]^{2/3}$	$[-\ln(1-\alpha)]^{1/3}$
5	N and G (n = 4)	A_4	$4(1-\alpha)[-\ln(1-\alpha)]^{3/4}$	$[-\ln(1-\alpha)]^{1/4}$
		Deceleration curves		
6	Diffusion, 1D	D_1	$1/(2\alpha)$	α^2
7	Diffusion, 2D	D_2	$1/(\ln(1-\alpha))$	$(1-\alpha)\ln(1-\alpha)+\alpha$
8	Diffusion, 3D	D_3	$1.5/[(1-\alpha)^{-1/3}-1]$	$(1-2\alpha/3)-(1-\alpha)^{2/3}$
9	Diffusion, 3D	D_4	$[1.5(1-\alpha)^{2/3}][1-(1-\alpha)^{1/3}]^{-1}$	$[1-(1-\alpha)^{1/3}]^2$
10	Diffusion, 3D	D_5	$(3/2)(1+\alpha)^{2/3}[(1+\alpha)^{1/3}\text{-}1]^{-1}$	$[(1+\alpha)^{1/3}\text{-}1]^2$
11	Diffusion, 3D	D_6	$(3/2)(1-\alpha)^{4/3}[[1/(1-\alpha)^{1/3}]\text{-}1]^{-1}$	$[[1/(1-\alpha)]^{1/3}\text{-}1]^2$
12	Contracted geometry shape (cylindrical symmetry)	R_2	$3(1-\alpha)^{2/3}$	$1\text{-}(1-\alpha)^{1/3}$
13	Contracted geometry shape (sphere symmetry)	R_3	$3(1-\alpha)^{2/3}$	$1\text{-}(1-\alpha)^{1/3}$
		Acceleration curves		
14	Mample power law	P_1	1	α
15	Mample power law (n = 2)	P_2	$2\alpha^{1/2}$	$\alpha^{1/2}$
16	Mample power law (n = 3)	P_3	$(1.5)\alpha^{2/3}$	$\alpha^{1/3}$
17	Mample power law (n = 4)	P_4	$4\alpha^{3/4}$	$\alpha^{1/4}$
18	Mample power law (n = 2/3)	$P_{3/2}$	$2/3(\alpha)^{-1/2}$	$\alpha^{3/2}$
19	Mample power law (n = 3/2)	$P_{2/3}$	$3/2(\alpha)^{1/3}$	$\alpha^{2/3}$
20	Mample power law (n = 4/3)	$P_{3/4}$	$4/3(\alpha)^{-1/3}$	$\alpha^{3/4}$

2.4.2. *Coats-Redfern method (18)*

The Coats-Redfern method is also an integral method, and it involves the thermal degradation mechanism. Using an asymptotic approximation for resolution of Equation 2, the following equation can be obtained:

$$\ln\left(\frac{g(\alpha)}{T^2}\right) = \ln\left(\frac{AR}{E\beta}\left(1-\frac{2RT}{E}\right)\right) - \frac{E}{RT} \qquad (5)$$

The expressions of $g(\alpha)$ for different mechanism have been listed in Table 2 (19, 20), and activation energy for degradation mechanism can be obtained from the slope of a plot of $\ln[g(\alpha)/T^2]$ vs. $1000/T$:

2.4.3. *Tang method (21)*

Taking the logarithms of sides and using an approximation formula for resolution of Equation 2, the following equation can be obtained:

$$\ln\left(\frac{\beta}{T^{1.894661}}\right) = \ln\left(\frac{AE}{Rg\ (\alpha)}\right) + 3.635041 - 1.894661\ \ln\ E - \frac{1.001450\,E}{RT} \qquad (6)$$

The plots of $\ln(\frac{\beta}{T^{1.89466\mathrm{T}}})$ vs. $1/T$ give a group of straight lines. The activation energy E can be obtained from the slope $-1.001450\ E/R$ of the regression line.

2.4.4. *Kissenger-Akahira-Sunose method (22)*

This method is integral isoconversional methods as FWO.

$$\ln\left[\frac{\beta}{T^2}\right] = \ln\left[\frac{AR}{E\,g(\alpha)}\right] - \frac{E}{RT} \qquad (7)$$

The dependence of $\ln(\beta/T^2)$ on $1/T$, calculated for the same α values at the different heating rates β can be used to calculate the activation energy.

2.4.5. *Determination of the kinetic model by master plots*

Using a reference at point $\alpha = 0.5$ and according to Equation 2, one gets:

$$g(\alpha) = \left(\frac{AE}{\beta\ R}\right)\ p(u_{0.5}) \qquad (8)$$

Where $u_{0.5} = E/RT$. When Equation 2 is divided by Equation 8, the following equation is obtained:

$$\frac{g(\alpha)}{g(0.5)} = \frac{p(u)}{p(u_{0.5})} \qquad (9)$$

Plots of $g(\alpha)/g(0.5)$ against α correspond to theoretical master plots of various $g(\alpha)$ functions (23, 24). To draw the experimental master plots of $P(u)/P(u_{0.5})$ against α from experimental data obtained under different heating rates, an approximate formula (25) of $P(u)$ with high accuracy is used $P(u) = \exp(-u)/[u(1.00198882u+1.87391198)]$. Equation 9 indicates that, for a given α, the experimental

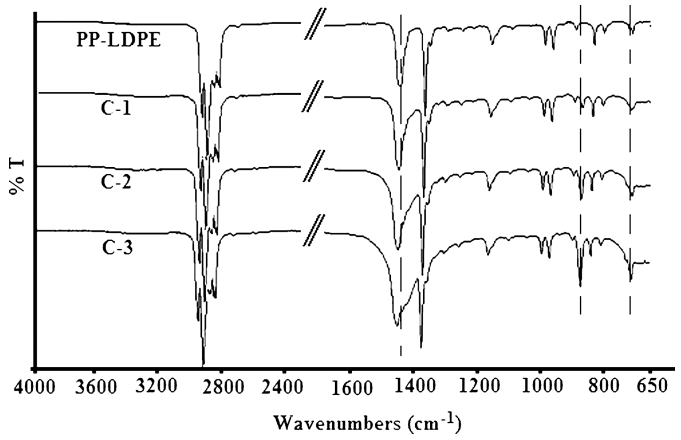

Fig. 1. FTIR spectra of blend PP-LDPE and composites C-1, C-2 and C-3.

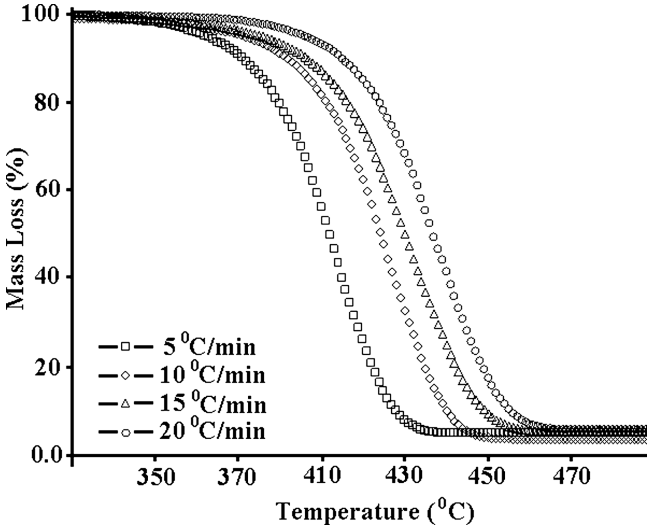

Fig. 2. TG curves of C-1 composite with $CaCO_3$ content 5 wt%.

value of g (α)/g($\alpha_{0.5}$) are equivalent when an appropriate kinetic model is used. Comparing the experimental master plots with theoretical ones can bring about the kinetic model (26).

3 Result and Discussion

3.1 Effect of $CaCO_3$ Filler Component on Blend PP/LDPE Structure

The FT-IR spectra of all compounds are shown in Figure 1. The IR spectrum as expected is quite simple and consisted of bands mainly corresponding to different vibration modes of C–C and C–H bonds. The IR spectrum of the samples recorded in the range 650–4000 cm^{-1} shows the characteristic absorption bands mainly at 2900 cm^{-1} (CH stretching) and 1460–1165 cm^{-1} (C-H bending and C–C stretching). But the change on some of the absorption peaks is minimal after modification. It is also observed that in Figure 1, C-1, C-2 and C-3 spectra gave to the bands at 1440, 874 and 712 cm^{-1}, which could be attributed asymmetric CO stretching, out-of-plane deformation of carbonate and OCO bending in-plane deformation vibrations of calcium carbonate, respectively. These newly infrared spectra bands were the characteristic FT-IR absorptions of calcium carbonate. By increasing the $CaCO_3$ filler component's weight increases the intensity of peaks. The results indicated that $CaCO_3$ dispersed completely in the blend.

3.2 Thermal Decomposition Process

Thermal degradation curves at different heating rates: 5, 10, 15, and 20°C min^{-1} under 10 mL min^{-1} nitrogen gas are given in Figures 2, 3, and 4. These TG curves correspond to a single-stage decomposition reaction where the procedural decomposition temperatures, such as initial and final temperatures, are well defined. The typical dynamic all TG curves of composites showed that the thermal decomposition took place mainly in one stage and the curves shifted to the right-hand side with the heating rate. It was also shown that the increasing $CaCO_3$ filler component in composites increased residue weight and thermal stability. The initial decomposition temperature of composites C-1, C-2 and C-3 was found to be 359, 363 and 367°C at 5°C min^{-1} in heating rate, respectively.

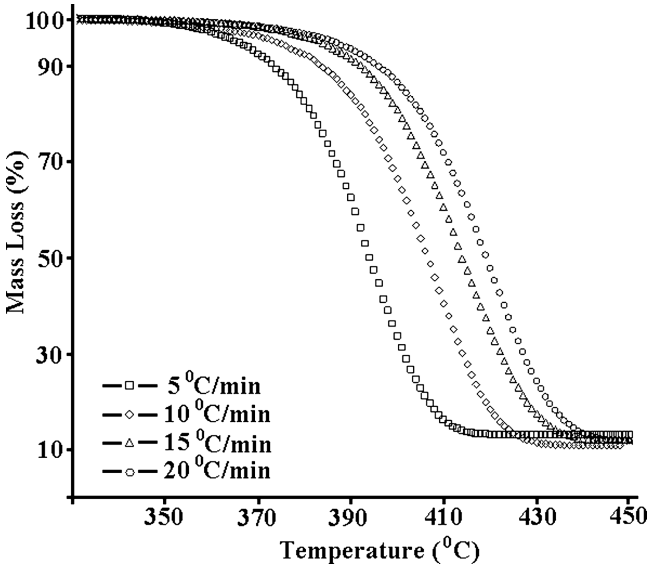

Fig. 3. TG curves of C-2 composite with $CaCO_3$ content 10 wt%.

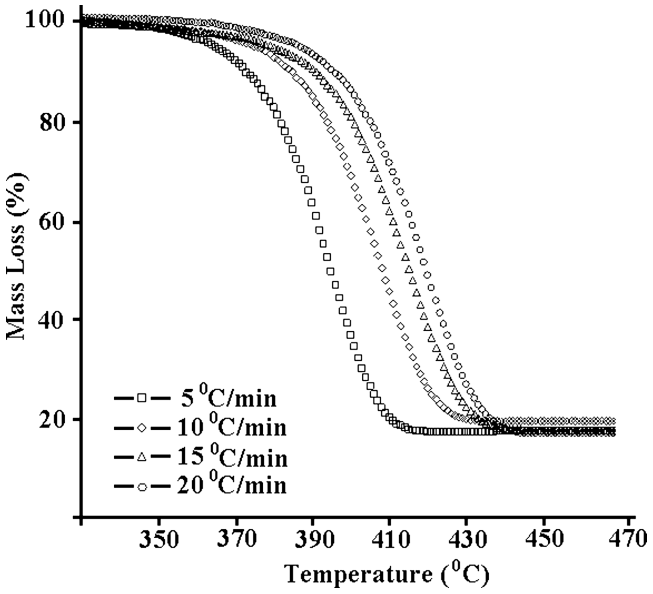

Fig. 4. TG curves of C-3 composite with $CaCO_3$ content 20 wt%.

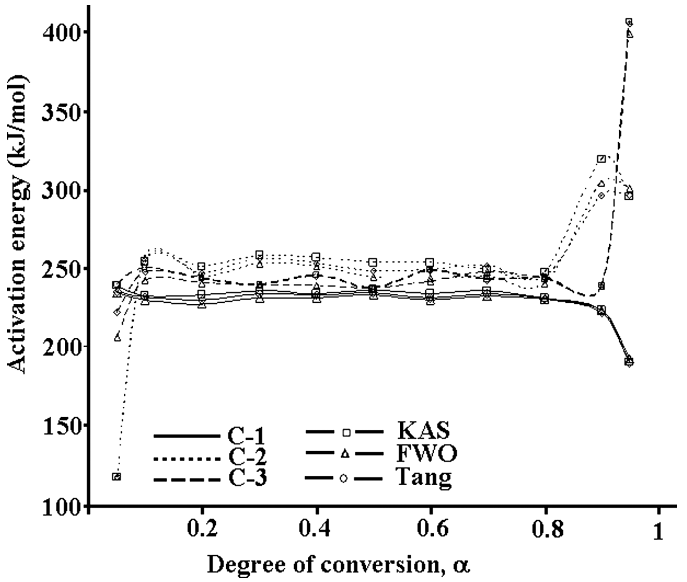

Fig. 6. Activation energy (E) as a function of conversion degree for the decomposition processes of composite C-1, C-2, and C-3 calculated by Tang, KAS and FWO methods.

3.3 Determination of Activation Energy Ea, Kinetic Model g(α), and Pre-exponential Factor A

For the study on the kinetics of thermal degradation of composites C-1, C-2 and C-3, we can select the isothermal thermogravimetry or the thermogravimetry at various heating rates. The isothermal thermogravimetry is superior to obtain accurate activation energy for thermal degradation, although it is time-consuming. In the case of thermal degradation of composites, the isoconversional methods based on TG at various heating rates is much more convenient than isothermal thermogravimetry for the investigation of thermal degradation kinetics, because it is independent of any thermodegradation mechanisms. Therefore, in the present work TG curves at various heating rates were obtained and the activation energies (Ea) for thermal degradation of polymer networks were calculated by Tang, KAS, FWO, and CR's plot, which are widely used methods. CR method was based on a single heating rate, while the other methods were based on multiple heating rates. According to the method of Tang, the apparent thermal degradation activation energies of composites, E_a, can be determined from the TG curves under different heating rates, such as in Figures 2, 3 and 4. According to Equation 6, activation energies of degradation can be determined from the slope of the linear relationship between $\ln(\beta/T^{1.894661})$ and $1000/T$, as shown in Figure 5 given for composite C-1 at varying conversion. The mean values of the activation energies of the thermal decomposition of composites C-1, C-2 and C-3

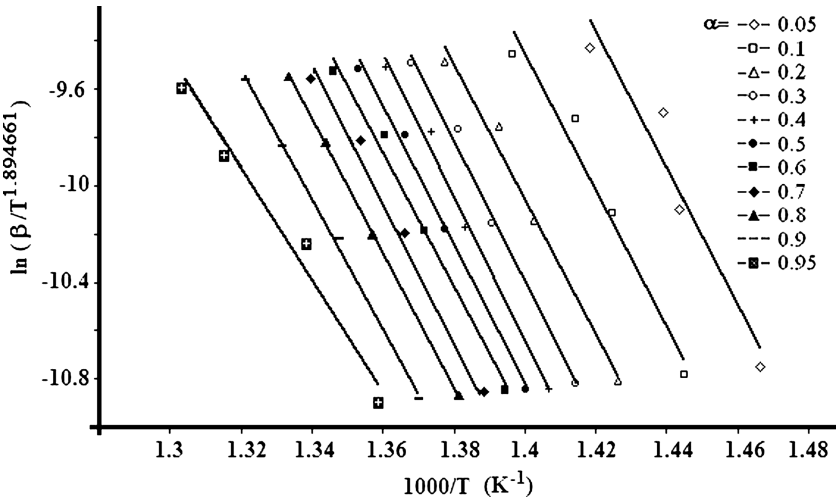

Fig. 5. Tang plots of composite C-1 for decomposition stage at varying conversation in N_2.

Table 3. Activation energies obtained by Tang, KAS and FWO methods of the composites

	C-1			*C-2*			*C-3*		
Alpha	*Tang*	*KAS*	*FWO*	*Tang*	*KAS*	*FWO*	*Tang*	*KAS*	*FWO*
0.05	238.8	234.9	234.2	117.8	117.3	156.5	239.6	222.0	206.1
0.1	232.3	231.7	230.0	253.7	253.0	256.6	250.3	247.4	242.3
0.2	233.2	230.0	226.8	250.5	246.5	244.6	243.4	242.8	239.9
0.3	235.9	233.7	231.2	258.0	256.0	252.6	239.6	239.1	238.6
0.4	234.0	232.9	230.8	256.6	252.9	250.5	245.3	244.7	239.2
0.5	236.5	234.5	232.9	253.5	248.4	244.5	237.7	237.1	237.0
0.6	234.0	231.2	229.7	253.5	248.9	243.8	248.6	248.0	241.5
0.7	236.0	233.7	232.4	249.0	251.4	244.6	242.6	241.9	247.3
0.8	230.7	230.2	230.4	247.2	244.4	240.0	244.2	243.6	243.2
0.9	222.8	222.2	223.0	318.7	296.0	303.9	239.1	238.5	238.4
0.95	190.7	190.0	192.6	295.4	296.2	300.8	405.7	405.0	398.4
Mean	229.5	227.7	226.7	250.4	246.4	248.9	257.8	255.5	252.0

in N_2 were 229.5, 250.4 and 257.8 mol^{-1} kJ/mol, respectively. The calculated results were summarized in Table 3.

Other iso-conversion methods used in this paper were that of KAS and FWO. According to the KAS method, Equation 7 was utilized to determine the values of activation energy from plots of $\ln(\beta/T^2)$ against $1000/T$ over a wide range of conversion. FWO method is also an integral method, also being independent of the degradation mechanism. According to Equation 4, the apparent activation energy of composites can be obtained from a plot of log β against $1000/T$ for a fixed degree of conversion since the slope of such a line given by $-0.456E/RT$. For each method, conversion degree, $\alpha = 0.05$, 0.1, 0.2, 0.3, 0.4, 0.5, 0.6, 0.7, 0.8, 0.9, 0.95 were chosen to evaluate E values of all the composites. The determined activation energies were listed in Table 3 and according to the KAS and FWO methods, the values of average activation energy for the thermal degradation of composites C-1, C-2 and C-3 were 227.7, 246.4, and 255.5 kJ mol^{-1} and 226.7, 248.9, and 252.0 kJ mol^{-1}, respectively, over the range of α given. This result agrees better with the mean values of activation energy obtained by the Tang method.

Constant mass loss lines were determined by measuring the temperature at a given mass percent for each heating

Table 4. Activation energies and pre-exponential factors for decomposition stage of C-1 obtained by CR method in N_2 atmosphere

	5° C min^{-1}		*10° C min^{-1}*		*15° C min^{-1}*		*20° C min^{-1}*	
	E (kJ mol^{-1})	*lnA*	*E (kJ mol^{-1})*	*lnA*	*E (kJ mol^{-1})*	*lnA*	*E (kJ mol^{-1})*	*lnA*
A_1	318.8	52.31	317.2	51.82	282.6	45.94	306.5	49.72
$A_{1,5}$	208.6	33.46	207.4	40.26	184.4	29.52	200.2	32.15
A_2	153.5	23.94	152.62	24.03	135.2	21.19	147.1	23.20
A_3	98.43	14.28	97.76	14.56	86.16	12.76	94.02	14.26
A_4	70.88	9.305	70.33	9.680	61.59	8.437	67.46	9.615
D_1	474.2	77.54	474.7	76.98	419.4	67.44	452.3	72.47
D_2	520.2	84.93	519.8	84.13	460.6	73.88	497.3	79.46
D_3	540.2	86.95	539.4	86.02	478.6	75.49	517.1	81.28
D_4	581.5	94.20	579.9	93.01	515.0	81.91	558.0	88.25
D_5	434.6	68.28	435.39	67.89	384.0	59.07	414.0	63.67
D_6	727.6	119.7	722.6	117.6	648.1	104.5	702.9	112.7
R_2	269.7	42.93	269.2	42.76	238.3	37.55	257.9	40.70
R_3	284.9	45.20	284.0	44.94	251.9	39.52	272.8	42.86
P_1	231.3	36.76	231.2	36.82	203.6	32.17	220.0	34.86
P_2	109.7	15.99	109.7	16.30	95.78	14.15	103.9	15.67
P_3	69.22	8.860	69.15	9.305	59.83	7.927	65.21	9.059
P_4	48.97	5.176	48.87	5.686	41.85	4.691	45.84	5.633
$P_{3/2}$	352.7	57.21	353.0	56.97	311.5	49.88	336.2	53.73
$P_{2/3}$	150.2	20.68	150.2	16.30	131.7	20.23	142.6	24.43
$P_{3/4}$	170.4	26.42	170.5	26.63	149.7	23.23	162.0	25.33

Table 5. Activation energies and pre-exponential factors for decomposition stage of C-2 obtained by CR method in N_2 atmosphere

	5° C min^{-1}		*10° C min^{-1}*		*15° C min^{-1}*		*20° C min^{-1}*	
	E (kJ mol^{-1})	*lnA*	*E (kJ mol^{-1})*	*lnA*	*E (kJ mol^{-1})*	*lnA*	*E (kJ mol^{-1})*	*lnA*
A_1	268.2	43.55	258.6	42.39	251.5	40.69	262.5	42.51
$A_{1,5}$	174.8	27.55	168.4	26.68	163.6	25.97	170.9	27.30
A_2	128.2	19.45	123.3	16.64	119.7	18.52	125.1	19.58
A_3	81.55	11.22	78.24	11.11	75.80	13.21	79.40	11.69
A_4	58.22	7.010	55.70	7.072	53.83	7.017	56.51	7.717
D_1	398.8	64.69	385.1	62.08	372.5	5969	388.7	62.23
D_2	439.9	71.25	424.7	68.66	411.7	65.76	429.5	68.53
D_3	457.0	72.76	441.2	69.67	428.0	67.07	446.5	69.93
D_4	492.0	78.90	474.9	75.52	461.4	72.82	481.3	75.86
D_5	361.5	55.83	349.0	53.53	337.3	51.32	351.9	53.66
D_6	611.1	99.78	589.0	95.40	575.5	92.37	599.9	96.04
R_2	227.3	35.59	219.9	34.32	221.4	33.19	221.8	34.80
R_3	240.1	37.46	231.5	36.09	224.6	34.91	234.5	36.60
P_1	193.5	30.19	186.5	29.26	180.2	28.24	188.2	29.67
P_2	90.88	12.61	87.32	12.42	84.08	12.10	88.06	12.97
P_3	56.66	6.549	54.23	6.631	52.02	6.515	54.65	7.208
P_4	39.55	3.379	37.69	3.592	359.9	3.586	37.95	4.190
$P_{3/2}$	296.2	47.53	285.8	45.74	276.4	4403	288.5	46.02
$P_{2/3}$	125.1	18.57	120.4	18.11	116.1	17.55	121.4	18.60
$P_{3/4}$	142.2	21.51	136.9	20.90	132.1	20.24	138.1	21.36

rate. In Figure 5, the Arrhenius type plots of dynamic TG runs related to the thermal decomposition process, were shown for masses ranging from $\alpha = 0.05$ to 0.95 in N_2. The values of correlation coefficients of linearization curves related to thermal decomposition processes of composites C-1, C-2, and C-3 were approximately 1.00. The kinetic data obtained by different methods agree with each other.

In Figure 6, the values of activation energy vs. conversion degree obtained by methods above for all of the composites

Table 6. Activation energies and pre-exponential factors for decomposition stage of C-3 obtained by CR method in N_2 atmosphere

	5° C min^{-1}		*10° C min^{-1}*		*15° C min^{-1}*		*20° C min^{-1}*	
	E (kJ mol^{-1})	*lnA*	*E (kJ mol^{-1})*	*lnA*	*E (kJ mol^{-1})*	*lnA*	*E (kJ mol^{-1})*	*lnA*
A_1	272.1	44.27	258.4	41.74	261.8	42.47	271.4	43.97
$A_{1,5}$	170.5	27.18	176.9	28.28	177.5	28.04	168.2	26.55
A_2	130.1	19.83	123.1	18.82	124.8	19.47	129.6	20.34
A_3	82.86	11.48	78.12	11.03	79.22	11.51	82.3	12.25
A_4	59.21	7.201	55.59	7.009	56.40	7.503	55.72	8.109
D_1	401.5	65.20	378.8	60.79	388.0	62.36	401.5	64.31
D_2	443.9	72.00	419.9	67.22	428.5	68.69	443.7	70.84
D_3	461.7	73.62	437.1	68.70	445.5	70.12	461.3	72.33
D_4	497.9	79.97	472.2	74.77	480.0	76.04	497.3	71.54
D_5	363.2	56.18	343.3	52.18	351.3	53.77	363.4	55.52
D_6	621.3	101.6	592, 4	95.47	597.9	96.24	619.7	99.24
R_2	229.7	36.05	217.2	33.85	221.3	34.74	229.3	36.04
R_3	243.0	38.00	230.1	35.70	234.0	36.55	242.5	37.90
P_1	194.8	30.46	183.4	28.60	187.9	29.60	194.6	30.72
P_2	91.53	12.76	85.72	5.202	87.95	12.82	91.24	13.52
P_3	57.09	6.638	53.12	6.386	54.61	7.005	56.77	7.586
P_4	39.87	3.448	36.83	3.397	37.94	3.971	39.53	4.485
$P_{3/2}$	298.1	47.92	281.1	44.76	287.9	46.05	298.1	47.58
$P_{2/3}$	125.9	16.38	118.2	17.66	121.2	18.47	125.7	19.29
$P_{3/4}$	143.1	21.67	134.5	20.42	137.9	21.25	142.9	24.48

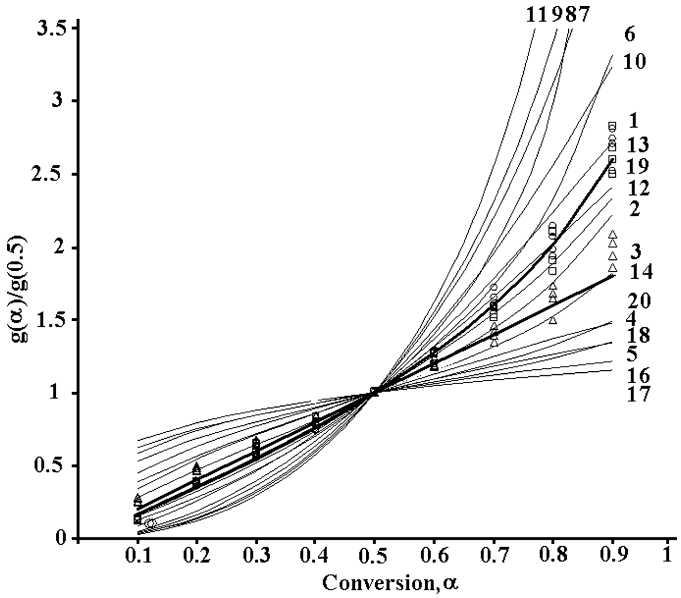

Fig. 7. Master plots of theoretical $g(\alpha)/g$ (0,5) against α for various reaction models (solid curves represent 20 kinds of reaction models given in Table 2) and experimental data [(○), (Δ) and (◇)] of composites at the heating rates 5, 10, 15 and 20°C min^{-1}.

were shown. The thermal decomposition of composites in N_2 presented the same behavior for the Tang, KAS and FWO methods. The initial activation energies required for thermal decomposition process of C-1, C-2, and C-3 was approximately 238.8, 117.8, and 239.6 kJ mol^{-1} according to the Tang method and the mean value of activation energy obtained by using the above methods for composite C-2 is smaller of that other two composites C-1 and C-3. The activation energy values for decomposition of each composites in the region of $0.1 < \alpha < 0.8$ is very close (Figure 5).

In order to find out the mechanism of the thermal decomposition of composites CR method has been chosen as it involves the mechanisms of the solid-state process. According to Equation 5, activation energy for every $g(\alpha)$ function listed in Table 2 can be calculated at constant heating rates from fitting of $\ln(g(\alpha)/T^2)$ vs. $1000/T$ plots. The activation energies and the pre-exponential factors at constant heating rates such as 5, 10, 15 and 20°C min^{-1} were tabulated in Tables 4, 5 and 6 for thermal degradation of composites. In order to determine the mechanism the degradation of composites agreed better with, we have compared the activation energies obtained by the methods above. According to Table 4, it could be found that the E values of composite C-1 in N_2 corresponding to mechanism P_1 had the best agreement with the values obtained by the Tang, FWO and KAS methods. Especially at the heating rate in 5°C min^{-1}, the activation energy corresponding to mechanism P_1 for thermal decomposition process stage is 231.3 kJ mol^{-1}, which was very close to the values of 227.7 kJ mol^{-1} obtained by the KAS method. The correlation coefficient was also much higher than other values.

As seen Table 5, the E values of composite C-2 obtained by KAS method is also in agreement with the value corresponding to mechanism R_3 at the heating rate in 5°C min^{-1}. According to Table 6, it can be seen that the thermal degradation process of composite C-3 corresponds to the mechanism R_3 which activation energy is 243.0 kJ mol^{-1}.

In order to confirm the conclusions, the experimental master plots $P(u)/P(u_{0,5})$ against α constructed from experimental data of the thermal degradation of composites under different heating rates and the theoretical master plots of various kinetic functions are all shown in Figure 7, The comparisons of the experimental master plots with theoretical ones indicated that the kinetic process of the thermal decomposition of the composites C-1, C-2 and C-3 agreed with the mechanisms P_1, and R_3 master curves very well, respectively.

By assuming P_1, and R_3 laws for all the composites, experimental data, the expression of the P_n and R_n models, and the average reaction energies predetermined were

Table 7. Pre-exponential factors and correlation coefficients obtained by plotting $\ln[\beta R/E]$-$\ln[P(u)]$ against kinetic functions

	Composite					
	C-1/P_1		*C-2/R_3*		*C-3/R_3*	
	Kinetic Function, $g(\alpha)$					
	$-ln(\alpha)$		*$-ln(1-(1-\alpha)^{1/3})$*		*$-ln(1-(1-\alpha)^{1/3})$*	
β ($K\,mol^{-1}$)	*ln A (s^{-1})*	*r*	*ln A (s^{-1})*	*r*	*ln A (s^{-1})*	*r*
5	36.96	0.9952	36.86	0.9864	39.96	0.9981
10	36.84	0.9962	37.96	0.9911	39.65	0.9902
15	36.93	0.9938	37.19	0.9823	39.71	0.9952
20	36.77	0.9964	36.96	0.9891	40.04	0.9891
mean	36.87		37.24		39.84	

r- Correlation coefficient.

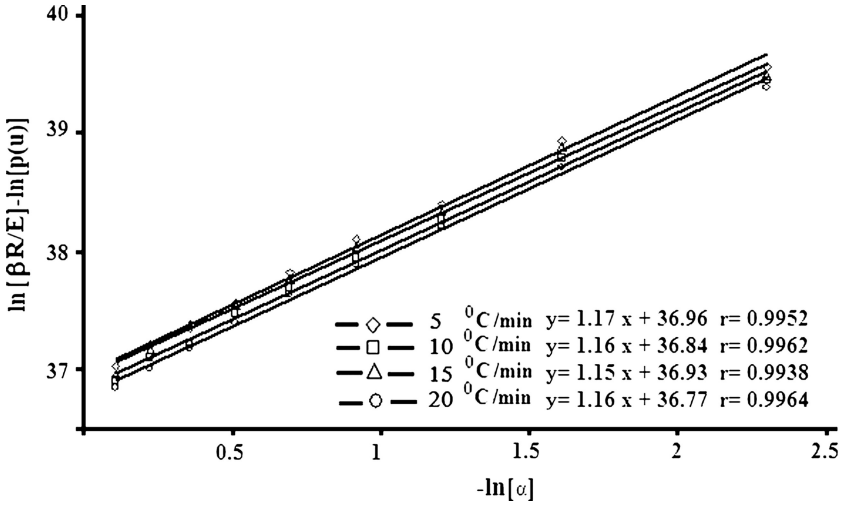

Fig. 8. Plotting ln[β R/E]-ln[$P(u)$] against – ln[α] for C-1 at different heating rates.

introduced into Equation 2, the following expression was obtained,

$$\ln[\beta R/\mathrm{E}] - \ln[P(u)] = \ln A - [\ln(\alpha)] \quad \text{for C-1} \tag{10}$$

$$\ln[\beta R/E] - \ln[P(u)] = \ln A - [\ln(1 - (1 - \mathrm{a})^{1/3})] \quad \text{for C-2} \tag{11}$$

$$\ln[\beta R/E] - \ln[P(u)] = \ln A - [\ln(1 - (1-\alpha)^{1/3})] \quad \text{for C-3} \tag{12}$$

A group of lines were obtained by plotting ln[$\beta R/E$]– ln[$P(u)$] against – ln[(α)] for *e.g*. C-1, As shown in Figure 8 and Table 7, the pre-exponential factors was calculated from the intercepts of the lines corresponding to various heating rates.

4 Conclusions

Polypropylene-Low Density Polyethylene blends containing different amount $CaCO_3$ filler component was prepared by melting-blend with a single-screw extruder. The effect of $CaCO_3$ filler component on thermal stability, thermal decomposition process and kinetic parameter such as activation energy, pre-exponential factor of prepared blends were investigated. The activation energies of the thermal degradation obtained by the Tang, KAS, FWO and Coats-Redfern methods in N_2 were found to be 229.5, 227.7, 226.7 and 231.3 kJ.mol^{-1} for composite C-1, 250.4, 246.4, 248.9, and 240.1 kJ.mol^{-1} for composite C-2, and 257.8, 255.5, 252.0 and 243.0 kJ.mol^{-1} for composite C-3. The resulting logarithmic values of the pre-exponential factor ln A (s^{-1}) obtained from master plots method were 36.87 for C-1, 37.24 for C-2 and 39.84 for C-3. Also, analysis of the results obtained by the Coats-Redfern method and master plots method show that the degradation mechanism of composites in N_2 goes to P_n and R_n mechanism for all stages of the decomposition. In conclusion, it was shown that the activation energy related to the decomposition of composites increased by the effect of increasing weight of $CaCO_3$ filler component. On the other hand, in terms of the Coats-Redfern method and master plot results, the decomposition process shows different mechanisms for blend with different CaCO3 contents. With $CaCO_3$ contents 5 wt% it shows P_n mechanism and with $CaCO_3$ contents 10 and 20 wt%, it shows R_n mechanism.

References

1. Paul, D.R. and Newman S. (1978) *Polymer Blends*, Academic Press: New York, Vol. 1, 1–33.
2. Tai, C.M., Li, R.K.Y. and Ng, C.N. (2000) *Polym. Test.,* 19, 143–154.
3. Li, J., Shanks, R.A., Olley, R.H. and Greenway, G.R. (2001) *Polymer*, 42, 7685–7694.
4. Stachurski, Z.H., Edward, G.H., Yin, M. and Long, Y. (1996) *Macromolecules*, 29, 2131–2137.
5. Chanda, M. and Roy, K.S. (2007) *Plastic Technology Handbook*, 4th Ed.; Taylor and Francis Group: Boca Raton, pp. 513–542.
6. Vasile, C. (2000) *Handbook of Polyolefins*, 2nd Ed.; Marcel Dekker: New York, pp. 175–185.
7. Yu, F., Zhang,H., Zheng, H., Yu, W. and Zhou, C. (2008) *Europ. Polym. Journ.,* 44, 79–86.
8. Shi, W.X., Li, Y.Y., Xu, J., Ma, G.G. and Sheng, J. (2007) *J. Macro. Sci., Part B*., 46(6), 1115–1126.
9. "irin, K. and Balcan, M., (2009) *Polym. Adv. Technol.* DOI: 10.1002/pat.1421
10. Shonaike, G.O. and Advani, S.G. (2003) *Advanced Polymeric Materials Structure Property Relationships*, CRC Press: New York, pp. 463–478.
11. Zhang, L., Wang, Z.H., Huang, R., Li, L.B. and Zhang, X.Y. (2002) *J Mater Sci.,* 37, 2615–2621.
12. Kolarik, J. and Jancar, J. (1992) *Polymer*, 33, 4961–4967.
13. Ma, C.G., Mai, Y.L., Rong, M.Z., Ruan, W.H. and Zhang, M.Q. (2007) *Composites Sci. and Techn*., 67, 2997–3005.
14. Gong, G., Xie, B.H., Yang, W., Li, Z.M., Lai, S.M. and Yang, M.B. (2006) *Polym. Test.*, 25, 98–106.
15. Flynn, J. and Wall, L. (1966) *Journal of Polym. Sci. Part B: Polym. Lett*., 4 (5), 323–328.

16. Ozawa, T. (1965) *Bull. Chem. Soc. Jpn*., 38, 881–886.
17. Doyle, C.J. (1961) *Appl. Polym. Sci*., 5, 285–292.
18. Coats, A.W. and Redfern, J.P. (1964) *Nature*, 201, 68–69.
19. Criado, J., Malek, J. and Ortega, A. (1989) *Thermochim Acta*., 147(2), 377–385.
20. Nunez, L., Fraga, F. and Villanueva, M. (2000) *Polymer*, 41(12), 4635–4641.
21. Tang, W., Liu, Y., Zhang, C.H. and Wang, C. (2003) *Thermochim Acta*, 408(1–2), 39–43.
22. Kissinger, H.F. (1957) *Anal. Chem*., 29, 1702–1706.
23. Gotor, F.J., Criado, J.M., Malek, J. and Koga, N. (2000) *J. Phys. Chem. A*., 104(46), 10777–10782.
24. Perez-Maqueda, L.A., Criado, J.M., Gotor, F.J. and Malek, J. (2002) *J. Phys. Chem. A*., 106(12), 2862–2868.
25. Wanjun, T., Yuwen, L., Hen, Z., Zhiyong, W. and Cunxin, W.J. (2003) *Therm. Anal. Cal.*, 74 (2), 309–315.
26. Tang, W., Liu, Y., Yang, X. and Wang, C. (2004) *Ind. Eng. Chem. Res*., 43(9), 2054–2059